



HAL
open science

Variability in the assessment of myocardial strain patterns: Implications for adequate interpretation

Nicolas Duchateau, Filip Loncaric, Maja Cikes, Adelina Doltra, Marta Sitges,
Bart Bijmens

► To cite this version:

Nicolas Duchateau, Filip Loncaric, Maja Cikes, Adelina Doltra, Marta Sitges, et al.. Variability in the assessment of myocardial strain patterns: Implications for adequate interpretation. *Ultrasound in Medicine & Biology*, 2020, 46, pp.244-254. hal-02350822

HAL Id: hal-02350822

<https://hal.science/hal-02350822>

Submitted on 6 Nov 2019

HAL is a multi-disciplinary open access archive for the deposit and dissemination of scientific research documents, whether they are published or not. The documents may come from teaching and research institutions in France or abroad, or from public or private research centers.

L'archive ouverte pluridisciplinaire **HAL**, est destinée au dépôt et à la diffusion de documents scientifiques de niveau recherche, publiés ou non, émanant des établissements d'enseignement et de recherche français ou étrangers, des laboratoires publics ou privés.

Variability in the assessment of myocardial strain patterns: Implications for adequate interpretation.

Running title: Variability in the assessment of myocardial strain patterns.

Nicolas Duchateau^a, Filip Loncaric^{b,c,d}, Maja Cikes^e, Adelina Doltra^{b,c,d}, Marta Sitges^{b,c,d}, Bart Bijmens^{f,g,h}.

^aCREATIS, CNRS UMR 5220, INSERM U1206, Université Lyon 1, France;

^bCardiovascular Institute, Hospital Clínic, Universitat de Barcelona, Spain;

^cInstitut d'Investigacions Biomèdiques August Pi i Sunyer (IDIBAPS), Barcelona, Spain;

^dCentro de Investigación Biomédica en Red Enfermedades Cardiovasculares (CIBERCV), Instituto de Salud Carlos III, Madrid, Spain;

^e Department of Cardiovascular Diseases, University of Zagreb School of Medicine and University Hospital Center Zagreb, Croatia;

^fUniversitat Pompeu Fabra, Barcelona, Spain;

^gICREA, Barcelona, Spain;

^hKU Leuven, Belgium.

Corresponding author:

Nicolas Duchateau

CREATIS, Université Lyon 1,

INSA Bâtiment Blaise Pascal

7 avenue Jean Capelle, 69621 Villeurbanne Cedex

Tel: +33.472437147

Email: nicolas.duchateau@creatis.insa-lyon.fr

Abstract

Variability in global and regional peak strain has been thoroughly studied, but not the variability in the spatiotemporal myocardial strain patterns. This study reports on such variability and its implications for adequate disease interpretation. Forty in-training operators were distributed on 20 workstations, and analyzed six cases with representative deformation patterns with commercial speckle-tracking. Inter-operator differences were quantified through the variability in myocardial delineations, spatiotemporal longitudinal strain patterns, and peak longitudinal strain. Intra-operator differences were assessed similarly using 10 repeated measurements from a single clinician expert. Delineations varied mainly along the lateral wall and at the valve level. Peak longitudinal strain variability was low to moderate. The spatiotemporal strain patterns were consistent despite high variability at the apex and near the valve. The results indicate that relevant pattern assessment is possible despite heterogeneous experience with speckle-tracking, and that careful interpretation of pattern abnormalities should be recommended before a more systematic quantitative analysis.

Keywords

Speckle-tracking; Myocardial strain; Spatiotemporal analysis; Reproducibility; Educational course.

Introduction

Myocardial strain is a valuable indicator to better understand cardiac mechanics on a wide range of diseases, and obtain reference values for diagnosis and prognosis (Amzulescu et al. 2019). However, its quantification from imaging data raises several concerns: validation of the software, standardization of the measurements, and interpretation of the results. Several efforts have been recently deployed to address the first two issues, in terms of definitions and computational aspects (Papachristidis et al. 2017; Voigt et al. 2015), and performance assessment (Alessandrini et al. 2016; De Craene et al. 2013; D'hooge et al. 2016).

Peak and timing values from global and regional strain have proven value over the ejection fraction (Cikes and Solomon 2016; Smiseth et al. 2016), and have been the main focus of standardization and reproducibility studies (Barbier et al. 2015; Cheng et al. 2013; Mirea et al. 2018a; Oxborough et al. 2012; Shiino et al. 2017). Nonetheless, a finer understanding of pattern changes with disease is highly recommended (Bijnens et al. 2009; Bijnens et al. 2012; Cikes and Solomon 2016; Fornwalt et al. 2009). The spatial distribution of myocardial motion and deformation (regionally or even locally) and their temporal evolution along the cycle provide complementary information that is missed by peak measurements (Cikes et al. 2010; Duchateau et al. 2011; Duchateau et al. 2014; Liu et al. 2016; McLeod et al. 2015; Parsai et al. 2009; Tabassian et al. 2017). Besides, the selection of peaks on challenging traces may be confusing (Anderson et al. 2008; Duchateau et al. 2014).

However, data about the local variability in the spatiotemporal deformation patterns (namely, at each point of the myocardium and each temporal instant) are missing. One may wonder to which extent the etiology-specific local strain abnormalities are preserved among operators, and what this could imply for disease interpretation.

In the context of a practical training course organized on a yearly basis, we set up a study to quantify the variability in a set of representative strain patterns measured by a large pool of operators with heterogeneous practice and profiles —clinicians and scientists. Our objectives were two-fold: (i) to report on the variability in spatiotemporal pattern observations and go beyond to the well-documented peak measurements —as explicitly required by the latest standardization initiatives (Mirea et al. 2018a) — and (ii) state on its implications for adequate disease understanding.

Materials and methods

Studied population

The course took place in 2018, and provided cases collected by the organizers during the past five years and covering a broad range of pathologies. Six representative cases with known deformation patterns were selected for this study: (1) a healthy adult individual, (2) a patient with cardiac amyloidosis (Cikes et al. 2010; Liu et al. 2016), (3a-3b) two athlete brothers with familial hypertrophic cardiomyopathy (Cikes et al. 2010; Liu et al. 2016), (4) a candidate for cardiac resynchronization therapy (CRT) with dilated cardiomyopathy and intra-ventricular dyssynchrony (Parsai et al. 2009), and (5) an athlete that died from sudden cardiac death. All echocardiographic examinations were performed in line with current international recommendations, and were recorded with a transthoracic probe (M4S or M5S, GE Healthcare, Milwaukee, WI, USA) using a commercially available system (Vivid 7 or 9, GE Healthcare, Milwaukee, WI, USA). The standard acquisition included both B-mode and tissue Doppler sequences, centered on the left ventricle, and Doppler flow analysis over the mitral and aortic valves. Additional sequences centered on the right ventricle were also acquired depending on the pathology. Machine settings (gain, time gain compensation, and compression) were adjusted for optimal visualization, including harmonic imaging. Frame rates of the analyzed sequences corresponded to standard acquisitions (Table 1).

The patients' and exam characteristics are summarized in Table 1. The analyzed cases were part of the clinical studies under investigation at the organizers' institutions, which complied with the Declaration of Helsinki and were accepted by the institutions' ethics committees, with written informed consent from all subjects.

Speckle-tracking analysis during the training course

Forty participants enrolled in the training course were distributed on 20 workstations equipped with a single commercial speckle-tracking tool (Echopac v.201, GE Healthcare, Milwaukee, WI, USA). Information on the participants' professional background and level of experience with speckle-tracking analysis was collected through a brief questionnaire at the beginning of the course. Results are summarized in Figure 1.

The participants were given training regarding the identification of mitral and aortic valve opening and closure on the Doppler sequences, manual delineation of the endocardial border on the B-mode sequence at end-systole, readjustments of delineations according to local wall thickness, and visual checking of the tracking quality—in particular at the apex and valve levels. After the initial training, the participants performed speckle-tracking analysis independently for each of the six cases. For consistency checking, the healthy case was analyzed both at the beginning and the end of the course. Myocardial segmentations and longitudinal strain

patterns were obtained from 4-chamber views using speckle-tracking on the left ventricle (LV) or the right ventricle (RV), depending on the studied case. To assess the intra-observer variability, a single expert clinician repeated the measurements 10 times in a row for each of the clinical cases one month after the training course. The cases were analyzed in random order to reduce bias in the analysis.

Statistical analysis of myocardial delineations and strain patterns

The output of speckle-tracking performed by the participants was exported through the “*store full trace*” option, which provides the position of all myocardial control points along the sequence, with spatial smoothing disabled in the software interface. The amount of exports saved during the course by participants is reported for each case in Table 2 and Figures 2, 3 and 4, and in the *Supplementary Material*.

The myocardial delineations and the spatiotemporal longitudinal strain patterns were obtained from these exported data using standard computations, implemented in Matlab (v.R2016, MathWorks, Natick, MA, USA). These computations included spatial resampling using cubic splines to compare the data at similar locations along the myocardium. As all participants processed the same sequence for each subject, no additional spatiotemporal alignment (Duchateau et al. 2011) of the data was required. No additional smoothing was added to the data. Drift compensation (forcing the values at the end of the cycle to match the ones at the onset of the cycle, option provided in the commercial speckle-tracking tool) was included in the results display.

Strain patterns were displayed using color-coded maps inspired from anatomical M-mode, where time (the cardiac cycle) is used as horizontal axis, and the spatial position along the myocardium is used as vertical axis. The color scale was centered on 0%, which corresponds to a lack of deformation, and red/blue colors stand for negative/positive strain corresponding to myocardial shortening/stretching.

Variability in the myocardial delineations was quantified at each point of the myocardial shape, by computing the covariance matrix of its 2D coordinates, and extracting the maximal variation as the square root of the first eigenvalue of this 2x2 matrix. This information was reported as the mean and maximum of these values over the whole myocardium, in millimeters.

Variability in the strain patterns was quantified through the standard deviation of strain values at each point of the myocardium and each instant of the cardiac cycle (bottom part of Figures 2 and 3). Strain variability is therefore expressed in absolute strain values (not relative) —a variability of 5% for -20% strain means that strain values roughly lie within the [-25% / -15%] interval. The median and inter-quartile range of strain patterns were also examined (central part of Figures 2 and 3). Intra-class correlation was not computed due to the varying

pool of raters who correctly exported the data for each studied case, and the small number of cases. Bland-Altman plots were not calculated for similar reasons, in addition to the high-dimensionality of the spatiotemporal strain patterns.

Differences in the strain patterns were further examined in two ways. First, abnormalities in the measurements were assessed at each point of the myocardium and each instant of the cardiac cycle, by computing the Mahalanobis distance between the strain pattern obtained by each operator and the strain patterns obtained by the rest of operators. This measure corresponds to the distance to the average pattern normalized by the pattern variability among operators. To better analyze the results, we computed the p-value associated to this distance, under the assumption that the distribution of strain values (at each point of myocardium and each instant of the cardiac cycle, among the pool of operators) is Gaussian, as done in our anterior works (Duchateau et al. 2011, Duchateau et al. 2012). Additionally, we estimated the maximum of the 2D normalized cross-correlation between the strain pattern obtained by each operator and the average strain pattern from the rest of operators, values of 0 and 1 meaning no correlation and perfect correlation, respectively.

The potential relation between the variability of the myocardial delineations and of the spatiotemporal strain patterns was assessed at each point of the myocardium by the Pearson correlation coefficient and its associated p-value, after averaging the inter- and intra-operator strain variability over time.

Finally, inter- and intra-operator variability in global and regional peak strain were quantified through the mean and standard deviation of peak strain values, expressed in percentages, after averaging the strain patterns over the whole myocardium or each segment and extracting the peak value of the averaged curve.

Results

To better understand the discussion around each processed case, snapshots of the speckle-tracking output and animated views of the tracked myocardium are provided as *Supplementary Material* (Figures S1 to S5). They are complemented by strain patterns from tissue Doppler acquisitions (Figures S3a and S3b) or motion assessment in anatomical M-mode (Figure S4), when relevant.

Variability in myocardial delineations

Figures 2 and 3 first illustrate the inter- and intra-operator variability in the myocardial delineations from the different participants and by an experienced clinician repeating the measurements. Delineations were made of 67 ± 8 points along the myocardium. They were rather consistent between participants, with a mean inter-operator

variability of 2.7 to 5.3 mm (maximal variability: 3.3 to 6.2mm). Main differences were observed along the lateral wall and at the valve level (for both LV and RV), and at the septal bulge level for the athlete case. For comparison, mean and maximal intra-operator variability was 1.3 to 2.9 mm and 1.9 to 5.4 mm, respectively. Delineations for the normal case were consistent between the beginning and the end of the course, with less outliers at the apex at the end of the course, but still substantial inter-operator variability over the lateral wall (mean inter-operator variability of 3.5 mm [before] against 3.8 mm [after], and 1.6 mm for the intra-operator measurements).

Observed strain patterns

Strain patterns are displayed in Figures 2 and 3. The black arrows and the overlaid numbers point out the main characteristics of the strain patterns, summarized as follows:

- Healthy adult (Figure S1 and subplots in Figures 2 and 3): Segmental strain curves reach a uniform peak value in the same timing. Shortening during systole and lengthening during early relaxation and atrial contraction are homogeneous over the myocardium. Some post-systolic thickening is present in the basal septum, while the signal quality is lower at the most basal part of the lateral wall close to the mitral ring resulting in an abnormal trace at this location.
- Amyloidosis (Figure S2 and subplots in Figures 2 and 3): A clear bilateral basal-apical gradient in strain values is present with near normal values in the apex and severely reduced basal strain (Cikes et al. 2010; Liu et al. 2016). This represents the typical “Japanese flag” appearance of the apical sparing.
- Athlete with hypertrophic cardiomyopathy and his brother (Figures S3a and S3b, and subplots in Figures 2 and 3): The LV looks enlarged and hypertrophic (see also Table 1), global strain is normal and most segments show normal deformation, but in both cases there is a region within the mid septum where deformation is much lower compared to both the direct proximal and distal regions (Cikes et al. 2010; Liu et al. 2016). This is confirmed by the strain pattern from tissue Doppler.
- CRT candidate with left bundle branch block (Figure S4 and subplots in Figures 2 and 3): The ventricle is dilated and the strain pattern is consistent with a dilated cardiomyopathy in the presence of a left bundle branch block, with characteristic spatial and temporal abnormalities. At the onset of the QRS complex, the septum quickly shortens while the lateral wall is being stretched. By the end of the QRS complex (while activation is still taking place) the lateral wall starts shortening, which results in a decreased speed of deformation of the septum, and the lateral segments continue to shorten after aortic valve closure. This

pattern has been described as a “septal flash” and is also recognizable on the anatomical M-mode image, with the fast inward-outward motion of the septum within the QRS complex, reduced systolic excursion during the rest of ejection and the presence of post-systolic shortening (Parsai et al. 2009). A complementary view on this pattern is given in Figure S8, with myocardial velocities in the radial direction using a display similar to Figures 2 and 3.

- Athlete that experienced sudden cardiac death (Figure S5 and subplots in Figures 2 and 3): This case shows an overall appearance of an athlete’s heart with bi-ventricular dilatation and hypertrophy (see also Table 1) and enlarged atria. When assessing RV deformation, a difference in basal and apical strain can be expected, but here a clear and unexpected decrease/absence of systolic shortening in the basal segment of the RV lateral wall can be observed. The present study is after a period of detraining where this abnormally low basal strain did not recover as compared to the assessment during training. The patient was recommended to decrease the intensity of sports, but died suddenly during running.

Variability in strain patterns

The bottom rows of Figures 2 and 3 illustrate the inter- and intra-operator variability of strain patterns, meaning the strain values at each point of the myocardium and each instant of the cycle. The maximal values for the inter-operator variability (maximal value observed in each strain variability map) ranged from 6.3 to 11.5%, mainly observed at the apex and the basal septal and lateral walls near the valve. The maximal values for the intra-operator variability ranged from 4.3 to 10.2%, also at these locations. Similarly to the myocardial delineations, the spatiotemporal strain patterns for the normal case were consistent between the beginning and the end of the course, with lower inter-operator strain variability at the apex at the end of the course, but still substantial inter-operator strain variability at the mitral valve level on both walls (maximal inter-operator variability of 8.9% [before] against 11.5% [after], against 6.0% for the intra-operator measurements). Low to moderate correlations were observed between the variability of the myocardial delineations and of the spatiotemporal strain patterns, as summarized in Figure 4.

The previously described pathology-specific strain abnormalities were visible in each of the six cases, consistently among participants regardless of the described inter-operator variability in myocardial delineations or strain patterns. Figure 5 confirms this by examining abnormalities and correlations in the measurements of the operators, and displaying the few strain patterns identified as outliers, which still allow identifying the main characteristics of each case.

For further consistency checking, we provide *Supplementary Material* Figures S6 and S7, similar to Figures 2 and 3 but for the course organized on the previous year (2017), which served as a feasibility study on four cases (normal, first brother athlete, septal flash, and athlete with sudden death) and led to similar observations.

Variability in global and regional peak strain measurements

To complement the analysis with more conventional measurements, the variability in global and regional peak longitudinal strain is summarized in Table 2. Both inter- and intra-operator peak strain variability (global: 0.7 to 1.5% [inter-operator] and 0.4 to 1.1% [intra-operator]; regional: 0.5 to 4.1% [inter-operator] and 0.2 to 4.0% [intra-operator]) were lower than the inter- and intra-operator variability in the strain patterns reported in the previous subsection.

Discussion

In this study, we compared the local deformation patterns quantified by a large pool of in-training operators with heterogeneous profiles and experience, and reported on the variability of the observations at each point of the myocardium and each instant of the cycle. Strain patterns were consistent among operators despite high inter-operator variability at specific locations (apex and near the valve on both walls). In particular, the etiology-specific local strain abnormalities were visible in all patterns and did not hamper disease interpretations.

In the last years, there have been several initiatives to better assess the variability and reproducibility of strain measurements. Clinical, industrial and academic instances put a lot of efforts to discuss and better harmonize segmentation and tracking techniques (Amzulescu et al. 2019; Papachristidis et al. 2017; Voigt et al. 2015). State-of-the-art algorithms were evaluated on synthetic echocardiographic images for which ground-truth myocardial delineation and deformation are known (Alessandrini et al. 2016; De Craene et al. 2013; D'hooge et al. 2016). Carefully designed studies also assessed specific aspects of reproducibility when measuring peak global and regional strain from commercial software (Barbier et al. 2015; Cheng et al. 2013; Mirea et al. 2018a; Oxborough et al. 2012; Shiino et al. 2017). In an educational perspective, the influence of the training level of the operators was also examined (Chan et al. 2017; Negishi et al. 2017; Yamada et al. 2014). In our study, the questionnaire about the participants' background and experience with speckle-tracking was anonymous, which precluded from investigating the quality of each operator's measurements against his/her experience.

In our study, the inter- and intra-operator variability in global and regional peak strain was rather low compared to the inter- and intra-operator variability in the strain patterns observable at specific locations. This is expected: peak measurements represent a single value along the cycle, not necessarily at the instant of highest variability, and encode strain values averaged over a region or the whole myocardium, which reduces differences between operators. While peak strain (either global or regional) is a practical measurement to situate a subject within a population or quantify its evolution, it disregards temporal dynamics more subtle to assess (e.g. the septal flash pattern from the CRT case presented here).

Several sources of variability (Mirea et al. 2018b) (number of control points, location of the control points, global and local thickness adjustments, etc.) were integrated into our evaluation, as participants had freedom to process the retained sequences. Acquisitions came from similar devices and were processed with the same tool, which limits differences in the measurements (Mirea et al. 2018a; Shiino et al. 2017). The analysis was done in 4-chamber views, which have lower regional peak strain variability compared to other views (Barbier et al. 2015). Nonetheless, the purpose of this paper is not to make a sensitivity analysis of the measurements against each of possible source of variability but to reflect operators' practice. In this sense, our pool of in-training operators was interesting due to their heterogeneous background, knowing that some of them can be more aware of the algorithmic techniques behind tracking, and others of the physiological traits of each case. Variability may therefore differ from the ranges obtained for expert operators with similar background, as in previous reproducibility studies (Barbier et al. 2015; Cheng et al. 2013). Nonetheless, we did not specifically investigate the correspondence between the inter-operator variability in the measurements and the professional background of the participants. The statistical significance of differences between the inter- and intra-operator variability in strain patterns was tested using the Levene's test and the Brown-Forsythe test at each point of the myocardium and at each temporal instant. Although some statistically significant differences were locally observed for some cases, the outcome of this test was difficult to interpret and arguable given the limited sample size, which is why this experiment was not reported in the manuscript.

Carefully examining the spatiotemporal strain patterns in light of their variability is explicitly recommended by the recent reproducibility assessment initiatives (Mirea et al. 2018a), but has not been addressed yet. Here, we examined this for the educational purposes of a training course and to open the discussion on how this could be approached in clinical practice. With this analysis, we do not aim at standardizing the operators' measurements. Instead, we help them develop a critical view on the output of the analysis. Nonetheless, key issues should be taught to limit uncertainties on the interpretation: minimum

knowledge on the processing techniques involved (what smoothing and drift compensation represent, what to expect from tracking in lower visible regions, what different number of control points or wider regions of interest may imply, does the tracking actually stick to the image, etc.), and careful understanding of the pathophysiology of the studied cases.

Limitations

This study was led within the guidance of a training course. This work is therefore different from a population study and has educational objectives. Although participants were free to perform the analysis in an independent way, the results were consistent between the beginning and the end of the course as exemplified on the normal case, even if no guarantee exists on their persistency afterwards. Within the context of the training course, we only included a limited set of cases in a 4-chamber view for illustration purposes. These cases had representative strain patterns that allowed examining the zones where variability between operators could be critical for interpretation. Similar observations were made for the other cases processed along the course, which covered ischemia, heart failure with preserved ejection fraction, and valve diseases, among others. Nonetheless, they had less representative strain patterns and the participants were therefore not asked to export their measurements for such cases. The selected data already depict a variety of common local shape and deformation abnormalities, including in regions subject to high inter- and intra-operator variability in the myocardial delineations and strain patterns (base and apex). Analyzing cases associated to different stages of a given disease was not performed.

Image quality may actually influence the accuracy of the results (Mirea et al. 2018b), but meets high standards in other reproducibility studies (Chan et al. 2017; Mirea et al. 2018a). Similarly, our study consisted of cases from the clinical routine of experienced echocardiographers, and had good image quality to pursue the course primary objectives.

Conclusion

Our study quantified the variability in spatiotemporal strain patterns on a substantial pool of in-training operators, which was not addressed before despite the value of the spatial and temporal strain abnormalities for disease understanding. We demonstrated that consistent pattern assessment is possible despite heterogeneous levels of experience with speckle-tracking. In light of minimum knowledge on the processing techniques involved and the pathophysiology of the studied cases, we actively recommend careful interpretation of abnormal deformation patterns in addition to systematic quantification of peak deformation values.

Acknowledgements

Funding: This work was partially supported by the Spanish Ministry of Economy and Competitiveness [grant TIN2014-52923-R; Maria de Maeztu Units of Excellence Programme - MDM-2015-0502] and FEDER, and the European Union H2020 programme [PIC H2020-MSCA-ITN-2017-764738].

Disclosures: In the recent years, MS received speaker fees from GE Healthcare, Toshiba, Medtronic, and Abbott; BB and MC received speaker fees from GE Healthcare. However, these did not influence the strain course related to this study, which was independently organized and not sponsored.

References

- Alessandrini M, Heyde B, Queiros S, Cygan S, Zontak M, Somphone O, Bernard O, Sermesant M, Delingette H, Barbosa D, De Craene M, O'Donnell M, Dhooge J. Detailed evaluation of five 3D speckle tracking algorithms using synthetic echocardiographic recordings. *IEEE Trans Med Imaging*. 2016;35:1915-26.
- Amzulescu MS, De Craene M, Langet H, Pasquet A, Vancraeynest D, Pouleur AC, Vanoverschelde JL, Gerber BL. Myocardial strain imaging: review of general principles, validation, and sources of discrepancies. *Eur Heart J Cardiovasc Imaging*. 2019;20:605-19.
- Anderson LJ, Miyazaki C, Sutherland GR, Oh JK. Patient selection and echocardiographic assessment of dyssynchrony in cardiac resynchronization therapy. *Circulation*. 2008;117:2009-23.
- Barbier P, Mirea O, Cefalù C, Maltagliati A, Savioli G, Guglielmo M. Reliability and feasibility of longitudinal AFI global and segmental strain compared with 2D left ventricular volumes and ejection fraction: intra- and inter-operator, test-retest, and inter-cycle reproducibility. *Eur Heart J Cardiovasc Imaging*. 2015;16:642-52.
- Bijnens BH, Cikes M, Claus P, Sutherland GR. Velocity and deformation imaging for the assessment of myocardial dysfunction. *Eur J Echocardiogr*. 2009;10:216-26.
- Bijnens BH, Cikes M, Butakoff C, Sitges M, Crispi F. Myocardial motion and deformation: What does it tell us and how does it relate to function? *Fetal Diagn Ther*. 2012;32:5-16.
- Chan J, Shiino K, Obonyo NG, Hanna J, Chamberlain R, Small A, Scalia IG, Scalia W, Yamada A, Hamilton-Craig CR, Scalia GM, Zamorano JL. Left ventricular global strain analysis by two-dimensional speckle-tracking echocardiography: the learning curve. *J Am Soc Echocardiogr*. 2017;30:1081-90.
- Cheng S, Larson MG, McCabe EL, Osypiuk E, Lehman BT, Stanchev P, Aragam J, Benjamin EJ, Solomon SD, Vasan RS. Reproducibility of speckle-tracking-based strain measures of left ventricular function in a community-based study. *J Am Soc Echocardiogr*. 2013;26:1258-66.e2.
- Cikes M, Sutherland GR, Anderson LJ, Bijnens BH. The role of echocardiographic deformation imaging in hypertrophic myopathies. *Nat Rev Cardiol*. 2010;7:384-96.
- Cikes M, Solomon SD. Beyond ejection fraction: an integrative approach for assessment of cardiac structure and function in heart failure. *Eur Heart J*. 2016;37:1642-50.
- De Craene M, Marchesseau S, Heyde B, Gao H, Alessandrini M, Bernard O, Piella G, Porras AR, Tautz L, Hennemuth A, Prakosa A, Liebgott H, Somphone O, Allain P, Makram Ebeid S, Delingette H, Sermesant

- M, D'hooge J, Saloux E. 3D strain assessment in ultrasound (Straus): a synthetic comparison of five tracking methodologies. *IEEE Trans Med Imaging*. 2013;32:1632-46.
- D'hooge J, Barbosa D, Gao H, Claus P, Prater D, Hamilton J, Lysyansky P, Abe Y, Ito Y, Houle H, Pedri S, Baumann R, Thomas J, Badano LP; EACVI/ASE/Industry Task Force to Standardize Deformation Imaging. Two-dimensional speckle tracking echocardiography: standardization efforts based on synthetic ultrasound data. *Eur Heart J Cardiovasc Imaging*. 2016;17:693-701.
- Duchateau N, De Craene M, Piella G, Silva E, Doltra A, Sitges M, Bijmens BH, Frangi AF. A spatiotemporal statistical atlas of motion for the quantification of abnormal myocardial tissue velocities. *Med Image Anal*. 2011;15:316-28.
- Duchateau N, Doltra A, Silva E, De Craene M, Piella G, Castel MÁ, Mont L, Brugada J, Frangi AF, Sitges M. Atlas-based quantification of myocardial motion abnormalities: added-value for understanding the effect of cardiac resynchronization therapy. *Ultrasound Med Biol*. 2012;38:2186-97.
- Duchateau N, Sitges M, Doltra A, Fernández-Armenta J, Solanes N, Rigol M, Gabrielli L, Silva E, Barceló A, Berruezo A, Mont L, Brugada J, Bijmens B. Myocardial motion and deformation patterns in an experimental swine model of acute LBBB/CRT and chronic infarct. *Int J Cardiovasc Imaging*. 2014;30:875-87.
- Fornwalt BK, Delfino JG, Sprague WW, Oshinski JN. It's time for a paradigm shift in the quantitative evaluation of left ventricular dyssynchrony. *J Am Soc Echocardiogr*. 2009;22:672-6.
- Liu D, Hu K, Nordbeck P, Ertl G, Störk S, Weidemann F. Longitudinal strain bull's eye plot patterns in patients with cardiomyopathy and concentric left ventricular hypertrophy. *Eur J Med Res*. 2016;21:21.
- McLeod K, Sermesant M, Beerbaum P, Pennec X. Spatio-temporal tensor decomposition of a polyaffine motion model for a better analysis of pathological left ventricular dynamics. *IEEE Trans Med Imaging*. 2015;34:1562-75.
- Mirea O, Pagourelas ED, Duchenne J, Bogaert J, Thomas JD, Badano LP, Voigt JU; EACVI-ASE-Industry Standardization Task Force. Variability and reproducibility of segmental longitudinal strain measurement: a report from the EACVI-ASE strain standardization task force. *JACC Cardiovasc Imaging*. 2018;11:15-24.
- Mirea O, Corîci OM, Berceanu M, Donoiu I, Militaru C, Istratoaie O. Variability of longitudinal strain measurements: levelling the playing field. *Acta Cardiol*. 2018;18:1-10.

- Negishi T, Negishi K, Thavendiranathan P, Cho G-Y, Popescu BA, Vinereanu D, Kurosawa K, Penicka M, Marwick TH; SUCCOUR Investigators. Effect of experience and training on the concordance and precision of strain measurements. *JACC Cardiovasc Imaging*. 2017;10:518-22.
- Oxborough D, George K, Birch KM. Intraobserver reliability of two-dimensional ultrasound derived strain imaging in the assessment of the left ventricle, right ventricle, and left atrium of healthy human hearts. *Echocardiography*. 2012;29:793-802.
- Papachristidis A, Galli E, Geleijnse ML, Heyde B, Alessandrini M, Barbosa D, Papitsas M, Pagnano G, Theodoropoulos KC, Zidros S, Donal E, Monaghan MJ, Bernard O, D'hooge J, Bosch JG. Standardized delineation of endocardial boundaries in three-dimensional left ventricular echocardiograms. *J Am Soc Echocardiogr*. 2017;30:1059-69.
- Parsai C, Bijmens B, Sutherland GR, Baltabaeva A, Claus P, Marciniak M, Paul V, Scheffer M, Donal E, Derumeaux G, Anderson L. Toward understanding response to cardiac resynchronization therapy: left ventricular dyssynchrony is only one of multiple mechanisms. *Eur Heart J*. 2009;30:940-9.
- Shiino K, Yamada A, Ischenko M, Khandheria BK, Hudaverdi M, Speranza V, Harten M, Benjamin A, Hamilton-Craig CR, Platts DG, Burstow DJ, Scalia GM, Chan J. Intervendor consistency and reproducibility of left ventricular 2D global and regional strain with two different high-end ultrasound systems. *Eur Heart J Cardiovasc Imaging*. 2017;18:707-16.
- Smiseth OA, Torp H, Opdahl A, Haugaa KH, Urheim S. Myocardial strain imaging: how useful is it in clinical decision making? *Eur Heart J*. 2016;37:1196-207.
- Tabassian M, Alessandrini M, Herbots L, Mirea O, Pagourelas ED, Jasaityte R, Engvall J, De Marchi L, Masetti G, D'hooge J. Machine learning of the spatio-temporal characteristics of echocardiographic deformation curves for infarct classification. *Int J Cardiovasc Imaging*. 2017;33:1159-67.
- Voigt JU, Pedrizzetti G, Lysyansky P, Marwick TH, Houle H, Baumann R, Pedri S, Ito Y, Abe Y, Metz S, Song JH, Hamilton J, Sengupta PP, Kolias TJ, d'Hooge J, Aurigemma GP, Thomas JD, Badano LP. Definitions for a common standard for 2D speckle tracking echocardiography: consensus document of the EACVI/ASE/Industry Task Force to standardize deformation imaging. *Eur Heart J Cardiovasc Imaging*. 2015;16:1-11.
- Yamada A, Luis SA, Sathianathan D, Khandheria BK, Cafaro J, Hamilton-Craig CR, Platts DG, Haseler L, Burstow D, Chan J. Reproducibility of regional and global longitudinal strains derived from two-

dimensional speckle-tracking and doppler tissue imaging between expert and novice readers during quantitative dobutamine stress echocardiography. *J Am Soc Echocardiogr.* 2014;27:880-7.

Table 1: Patient and exam characteristics

	Normal	Amyloid	Athlete Brother #1	Athlete Brother #2	CRT	Sudden death
General						
Frame rate (frames per second)	55	54	67	39	64	40
Age (y)	31	53	21	19	46	47
Sex	male	male	male	male	male	male
LV measurements						
Basal septal thickness (cm)	0.8	1.6	1.6	1.4	1.0	1.2
Posterior wall thickness (cm)	1.0	2.3	1.1	1.0	1.0	1.2
LV end-diastolic diameter (cm)	4.1	4.1	4.6	4.6	6.7	5.2
LV end-systolic diameter (cm)	3.3	3.0	2.6	3.2	6.3	4.5
LVED volume (ml)	98	88	101	85	178	149
LVES volume (ml)	40	30	34	30	131	65
LVEF (%)	60	66	66	65	26	56
E (m/s)	71	70	56	88	54	71
A (m/s)	66	33	24	58	67	51
E/A	1.09	2.12	2.36	1.52	0.82	1.39
Septal e' (m/s)	10	4	12	12	5	-
Septal a' (m/s)	10	5	7	7	8	-
Lateral e' (m/s)	-	7	17	18	6	17
Lateral a' (m/s)	-	11	7	6	4	6
E/e'	7.1	11.7	3.9	5.9	9	4.2

LV: left ventricle; ED: end-diastolic; ES: end-systolic; EF: ejection fraction; CRT: cardiac resynchronization therapy.

Table 2: Peak longitudinal strain: mean \pm standard deviation (%)

	Normal Before	Normal After	Amyloid	Athlete Brother #1	Athlete Brother #2	CRT	Sudden death
Inter-operator variability	N=16	N=15	N=15	N=20	N=16	N=13	N=16
Global	-14.3 \pm 1.2	-13.9 \pm 0.8	-8.9 \pm 0.7	-15.0 \pm 1.4	-18.3 \pm 1.5	-8.0 \pm 1.0	-15.0 \pm 1.0
Basal septal	-12.1 \pm 2.9	-12.0 \pm 2.6	-8.2 \pm 1.5	-15.2 \pm 2.4	-10.4 \pm 3.3	-9.7 \pm 1.7	-11.4 \pm 1.9
Mid septal	-16.5 \pm 0.5	-16.4 \pm 0.6	-9.9 \pm 0.7	-9.8 \pm 1.3	-18.4 \pm 0.9	-11.9 \pm 1.4	-16.0 \pm 0.7
Apical septal	-15.9 \pm 2.6	-15.5 \pm 2.4	-16.1 \pm 2.9	-23.1 \pm 3.7	-25.7 \pm 3.7	-14.7 \pm 3.0	-16.8 \pm 3.7
Apical lateral	-19.8 \pm 4.1	-19.3 \pm 2.1	-8.0 \pm 2.0	-14.4 \pm 2.5	-22.3 \pm 2.8	-13.9 \pm 2.7	-29.2 \pm 2.0
Mid lateral	-15.1 \pm 2.2	-14.1 \pm 2.0	-8.4 \pm 1.0	-16.1 \pm 2.1	-18.5 \pm 1.5	-5.9 \pm 2.9	-13.4 \pm 2.6
Basal lateral	-11.3 \pm 2.6	-10.9 \pm 4.0	-4.4 \pm 1.6	-14.0 \pm 2.7	-17.2 \pm 1.9	-10.0 \pm 2.4	-8.1 \pm 3.0
Intra-operator variability	N=10	-	N=10	N=10	N=10	N=10	N=10
Global	-15.2 \pm 0.4	-	-9.5 \pm 0.5	-16.5 \pm 0.7	-19.9 \pm 0.8	-7.8 \pm 1.1	-15.3 \pm 0.8
Basal septal	-11.5 \pm 1.7	-	-8.5 \pm 0.8	-16.1 \pm 1.4	-12.2 \pm 2.4	-9.9 \pm 0.9	-11.9 \pm 1.5
Mid septal	-16.4 \pm 0.4	-	-10.0 \pm 0.4	-11.2 \pm 0.6	-19.0 \pm 0.2	-11.5 \pm 1.4	-16.1 \pm 0.5
Apical septal	-20.6 \pm 1.4	-	-19.2 \pm 2.4	-26.6 \pm 1.8	-29.7 \pm 1.3	-16.3 \pm 1.7	-18.1 \pm 2.1
Apical lateral	-25.0 \pm 0.7	-	-8.6 \pm 0.8	-18.2 \pm 1.9	-24.0 \pm 1.3	-15.6 \pm 1.1	-30.2 \pm 1.4
Mid lateral	-15.3 \pm 1.0	-	-8.2 \pm 0.6	-16.4 \pm 1.3	-19.1 \pm 1.0	-6.4 \pm 0.8	-14.0 \pm 2.4
Basal lateral	-9.0 \pm 1.4	-	-4.5 \pm 1.1	-13.6 \pm 2.1	-16.8 \pm 1.6	-7.7 \pm 4.0	-8.4 \pm 1.8

CRT: cardiac resynchronization therapy.

Figure legends

Figure 1: Summary of the answers to the participants' survey, regarding their background and levels of experience in the analysis of cardiac images and their use of Echopac and speckle-tracking.

Figure 2: Inter-operator variability in myocardial delineations (*top*) and **strain patterns** (*central* part: median and first/third quartile strain patterns, *bottom* row: variability in strain patterns). (1) homogeneous pattern; (2) “Japanese flag”: preserved deformation only around the apex; (3) localized non-deforming region surrounded by more normal deformation; (4) intra-ventricular dyssynchrony with marked “septal flash”; (5) severely reduced RV basal lateral wall deformation. CRT: cardiac resynchronization therapy. Vertical dashed lines stand for the following events: Q1/Q2: onset of QRS; AVO/AVC/MVO/MVC: aortic/mitral valve opening/closure.

Figure 3: Intra-operator variability in myocardial delineations and strain patterns. Display similar to Figure 2.

Figure 4: Variability of the myocardial delineations against the variability of the strain patterns (at each point of the myocardium, after averaging the variability in strain patterns over time; similar trends observed when taking its maximal value over time). The Pearson correlation coefficient and its associated p-value are indicated in each subplot.

Figure 5: Consistency in the measurements among the operators. *Top* row: abnormality in the strain pattern obtained by each operator compared to the strain patterns obtained by the rest of operators (p-value associated to the Mahalanobis distance, averaged over the whole spatiotemporal pattern, and displayed in a logarithmic scale). *Central* row: maximal value of the 2D normalized cross-correlation between the strain pattern obtained by each operator and the average strain pattern from the rest of operators. *Bottom* part: strain patterns identified as outliers, to compare with the median and first/third quartile strain patterns from Figure 2. The p-value and correlation obtained are summarized in the top right corner of each pattern.

Supplementary Material

Supplementary videos

Video S1: normal control.

Video S2: patient with cardiac amyloidosis.

Video S3a: first brother athlete with familial hypertrophic cardiomyopathy.

Video S3b: second brother athlete with familial hypertrophic cardiomyopathy.

Video S4: idiopathic patient with dilated cardiomyopathy and intra-ventricular dyssynchrony
(presence of a “septal flash” including apical rocking).

Video S5: athlete with local right ventricular deformation abnormalities who died suddenly.

Supplementary figures

Figure S1: normal control. Longitudinal strain from speckle-tracking.

Figure S2: patient with cardiac amyloidosis. Longitudinal strain from speckle-tracking.

Figure S3a: first brother athlete with familial hypertrophic cardiomyopathy. *Top:* longitudinal strain from speckle-tracking. *Bottom:* longitudinal strain from tissue Doppler imaging.

Figure S3b: second brother athlete with familial hypertrophic cardiomyopathy. *Top:* longitudinal strain from speckle-tracking. *Bottom:* longitudinal strain from tissue Doppler imaging.

Figure S4: idiopathic patient with dilated cardiomyopathy and intra-ventricular dyssynchrony
(presence of a “septal flash” including apical rocking). *Top:* longitudinal strain from speckle-tracking. *Bottom:* anatomical M-mode highlighting the septal flash pattern. SF: septal flash; SE: systolic excursion; PSS: post-systolic shortening.

Figure S5: athlete with local right ventricular deformation abnormalities who died suddenly.
Longitudinal strain from speckle-tracking.

Figure S6: Inter-operator variability in myocardial delineations and strain patterns, from the previous year course. Display similar to Figure 2.

Figure S7: Intra-operator variability in myocardial delineations and strain patterns, from the previous year course. Display similar to Figure 2.

Figure S8: Inter-operator variability in velocity patterns in the radial direction for the normal and CRT cases. Display similar to Figure 2. The septal flash pattern is visible in the CRT case

(inward/outward motion of the septum during the isovolumic contraction), compared to the normal case (synchronous contraction/relaxation pattern between the septal and lateral walls). Again, variability exists between operators but still allows relevant assessment of the pattern abnormalities.

Figure 1

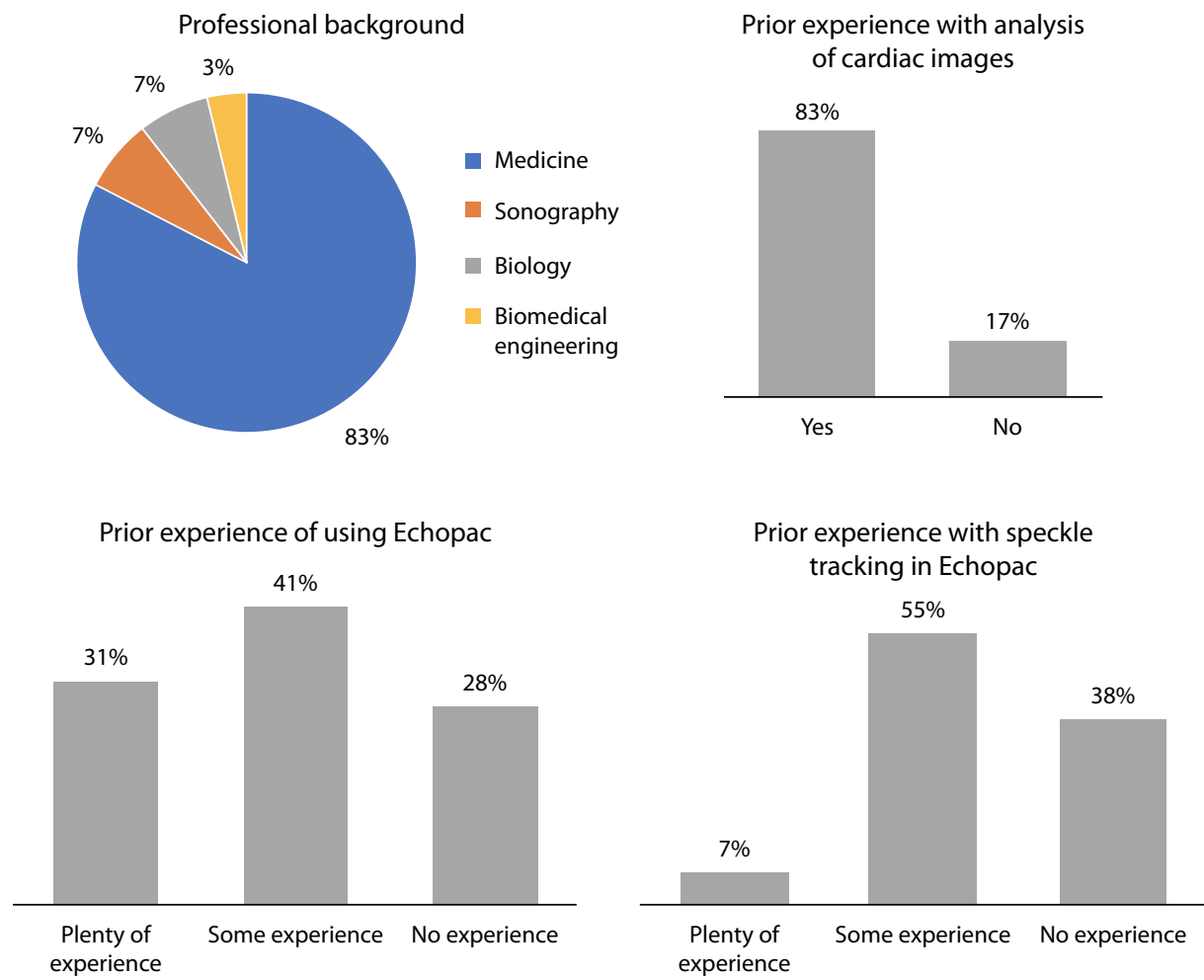


Figure 2

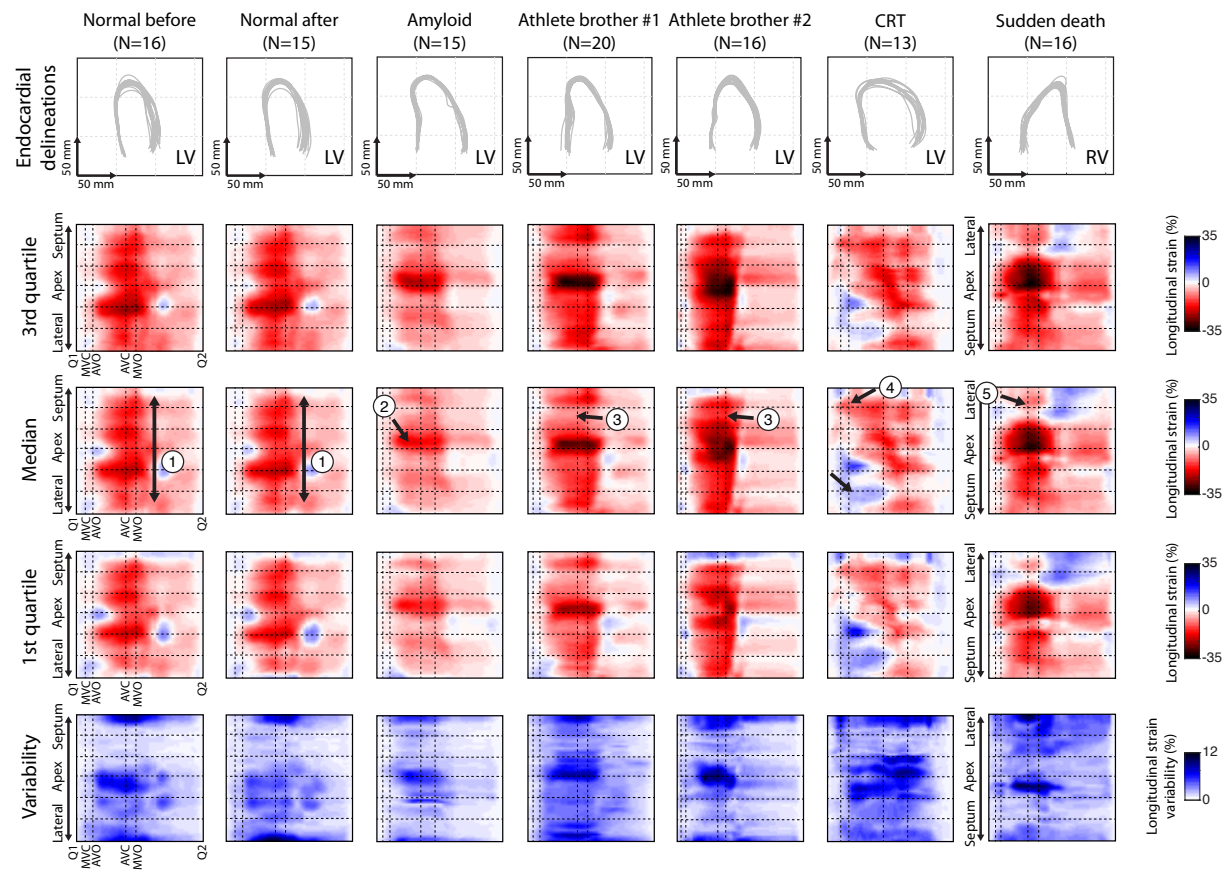


Figure 3

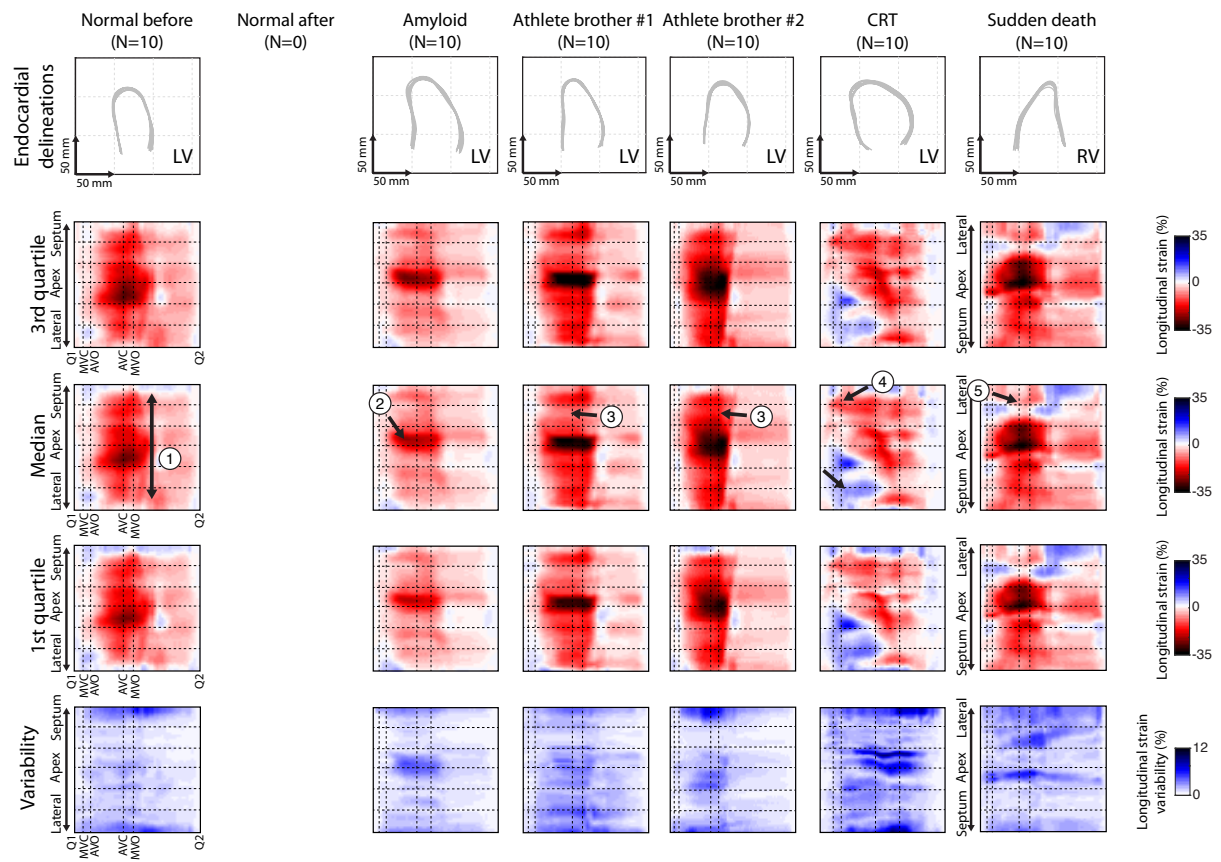


Figure 4

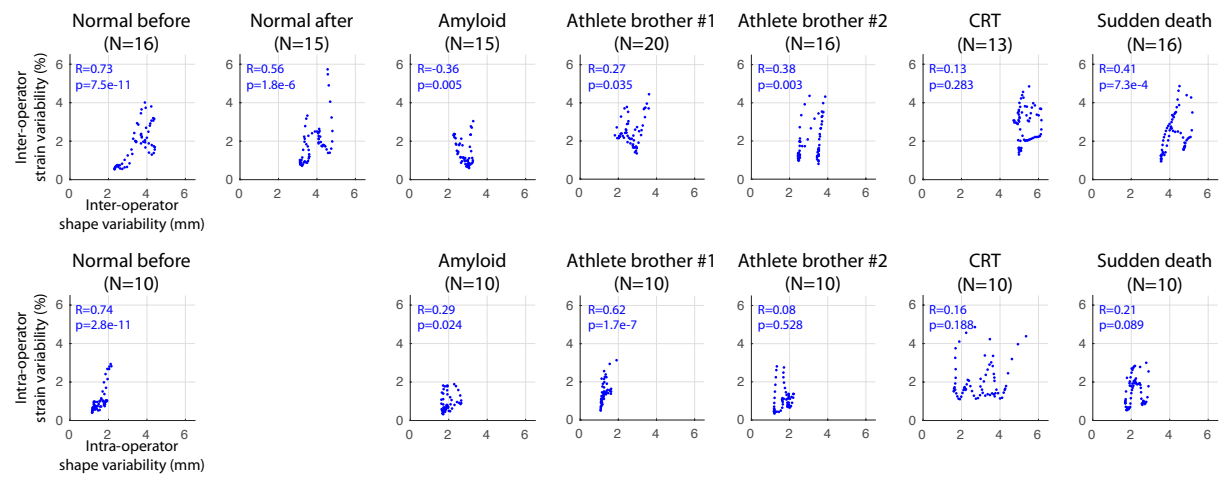


Figure 5

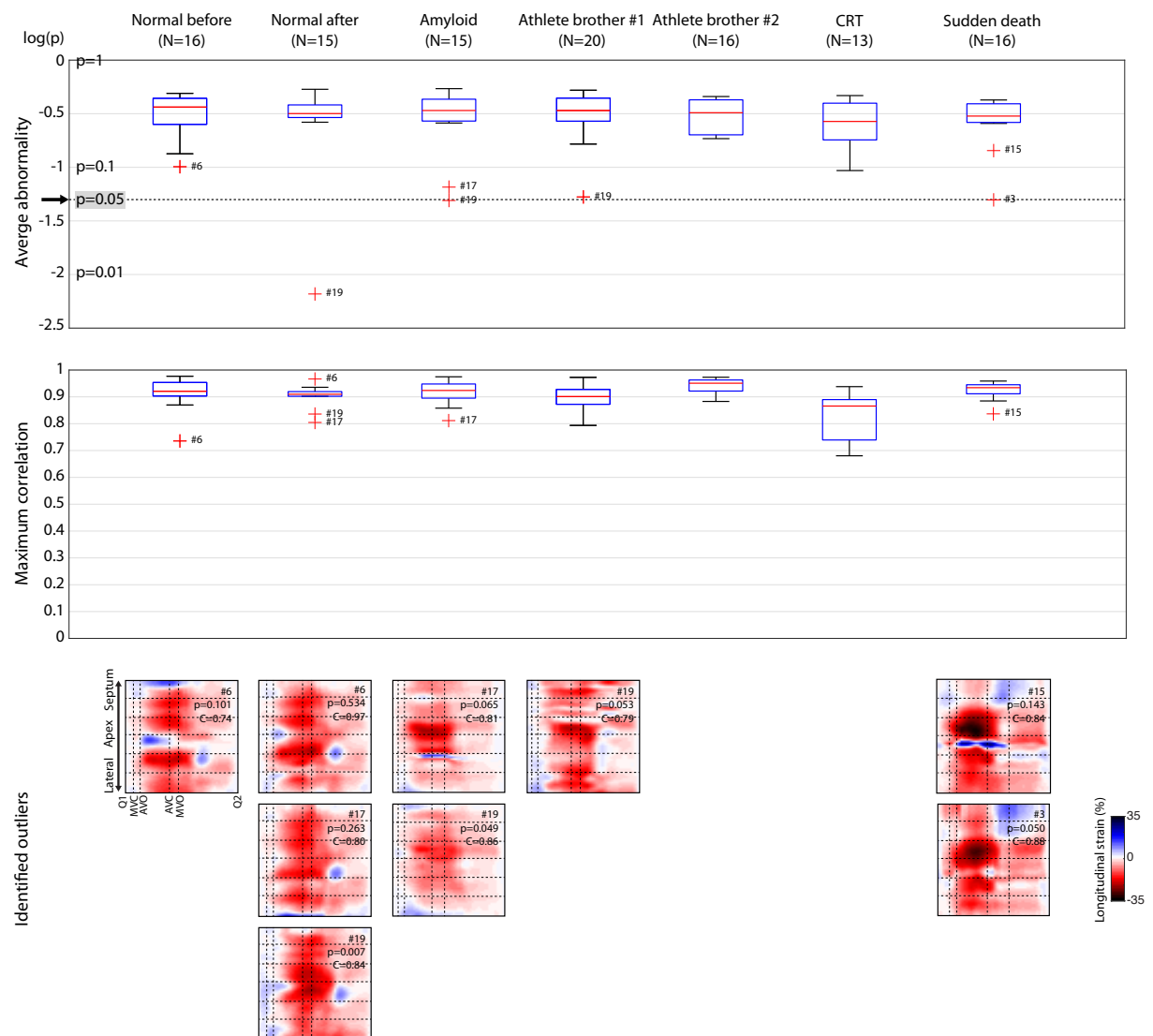


Figure S1

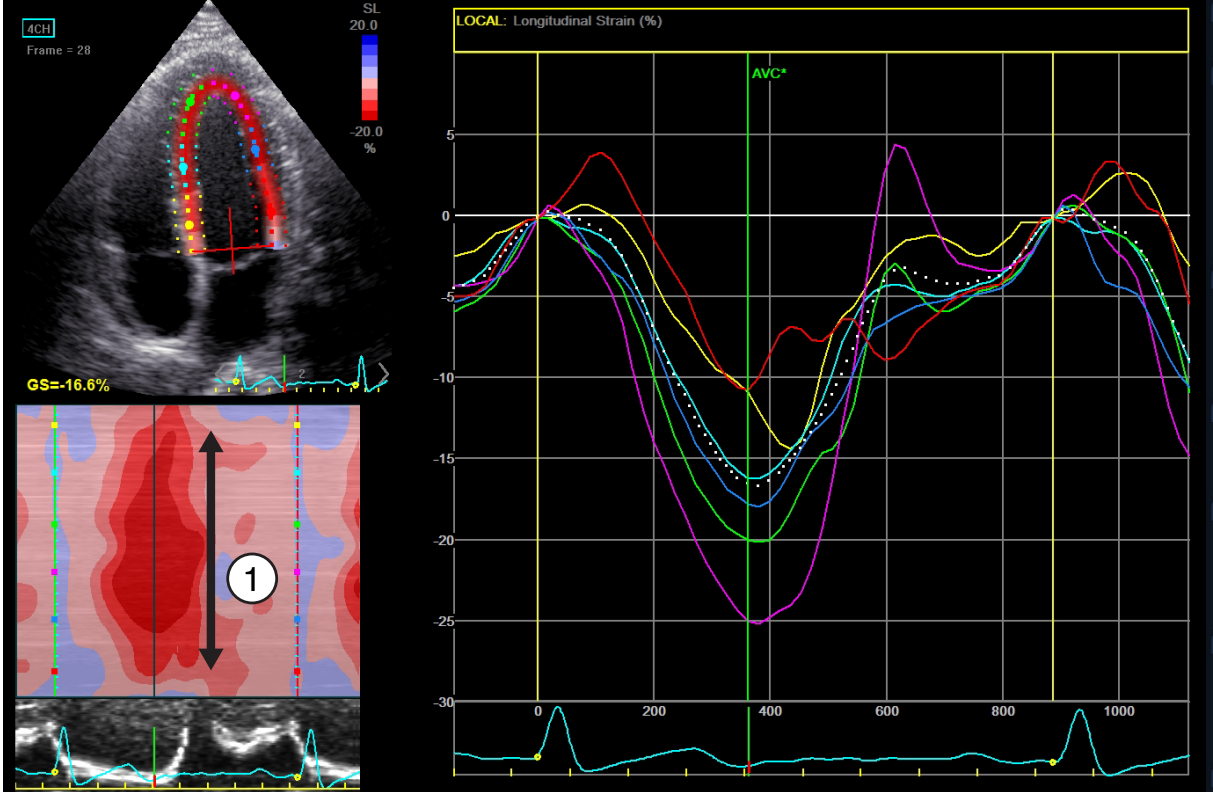


Figure S2

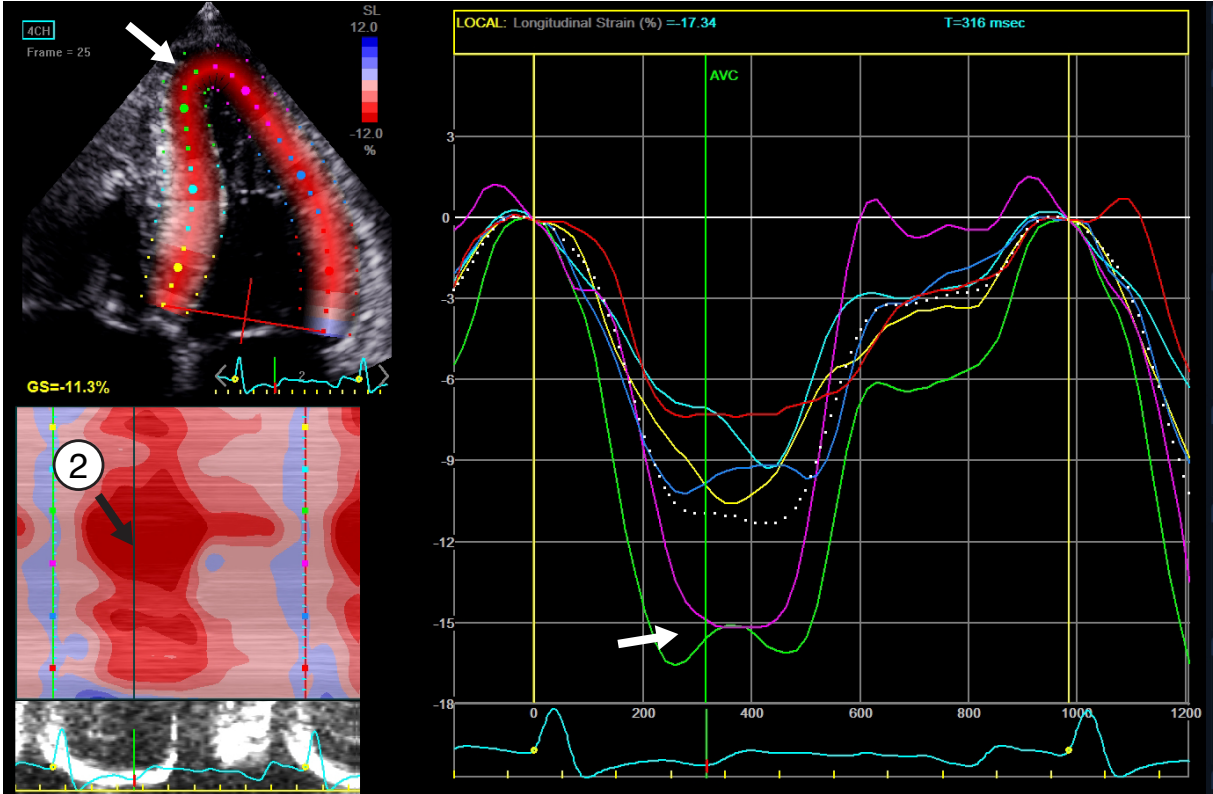


Figure S3a

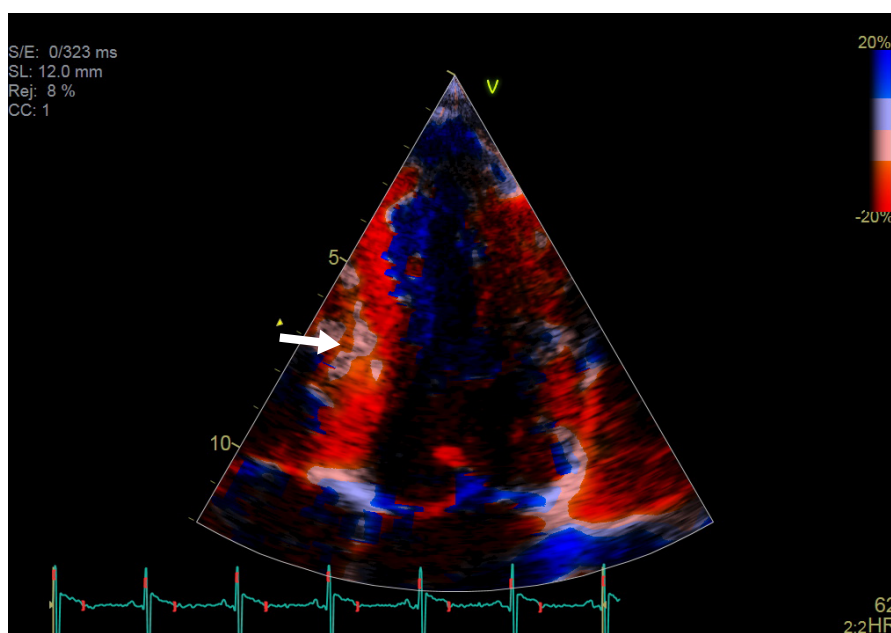
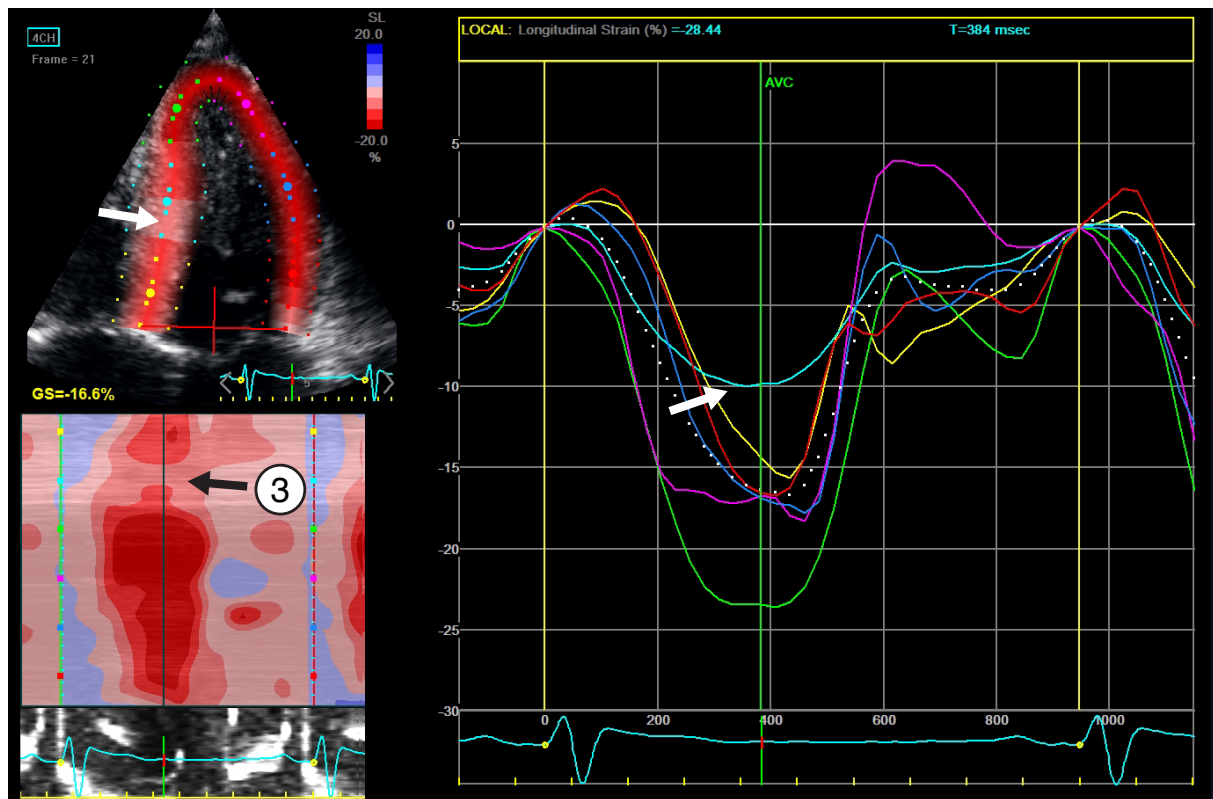


Figure S3b

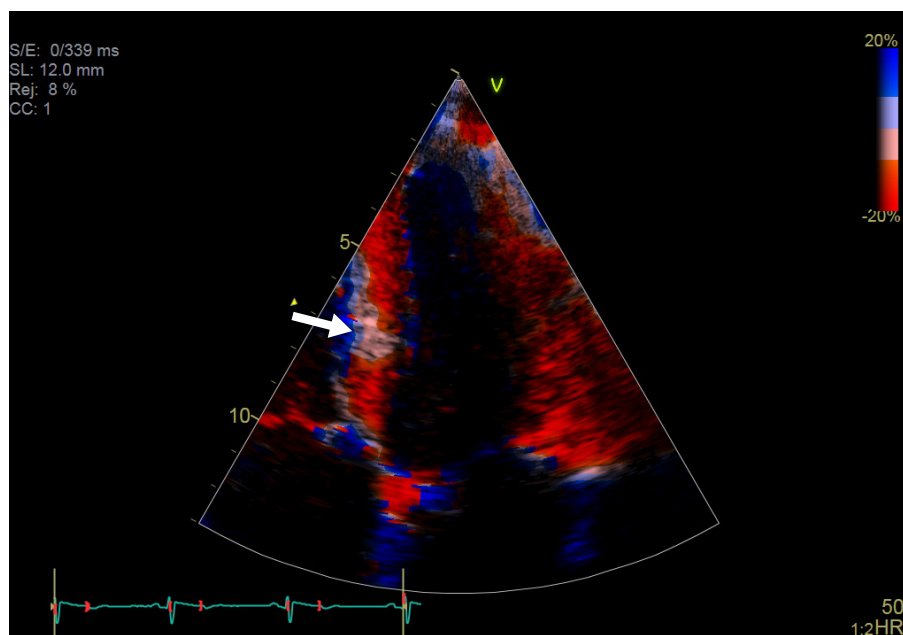
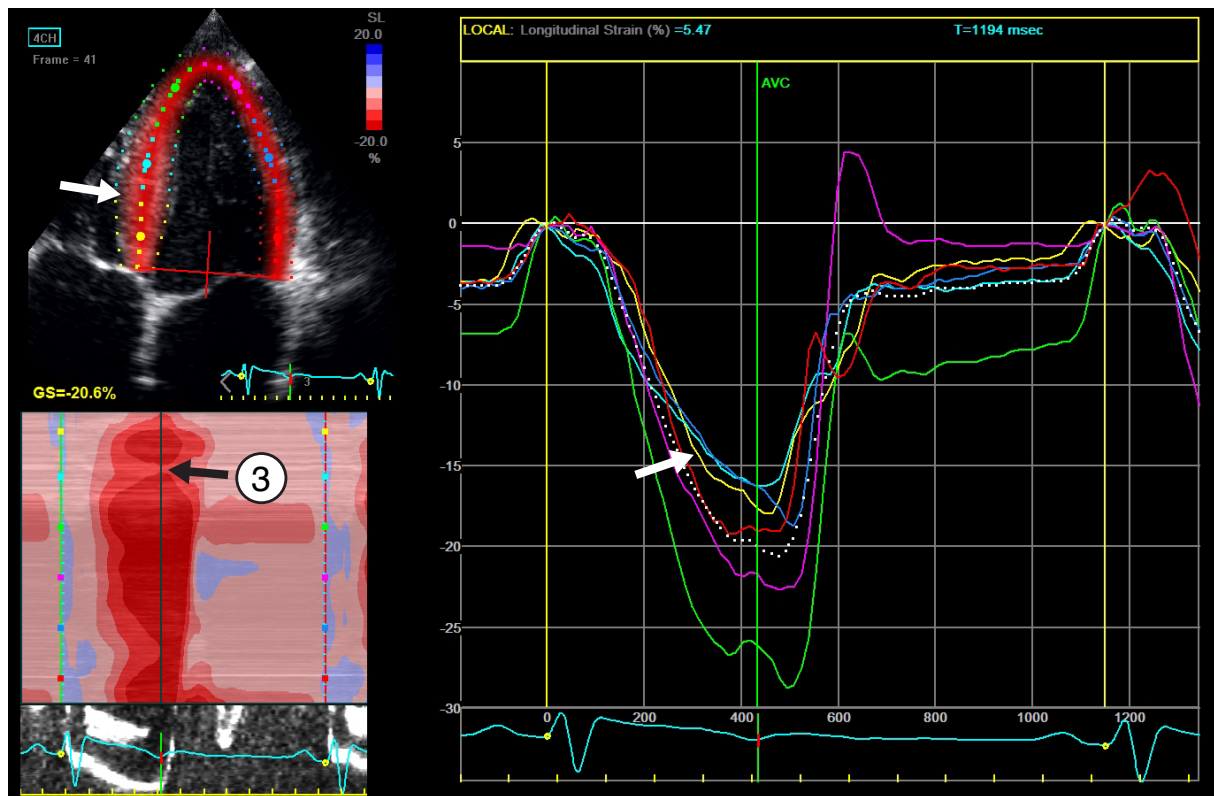


Figure S4

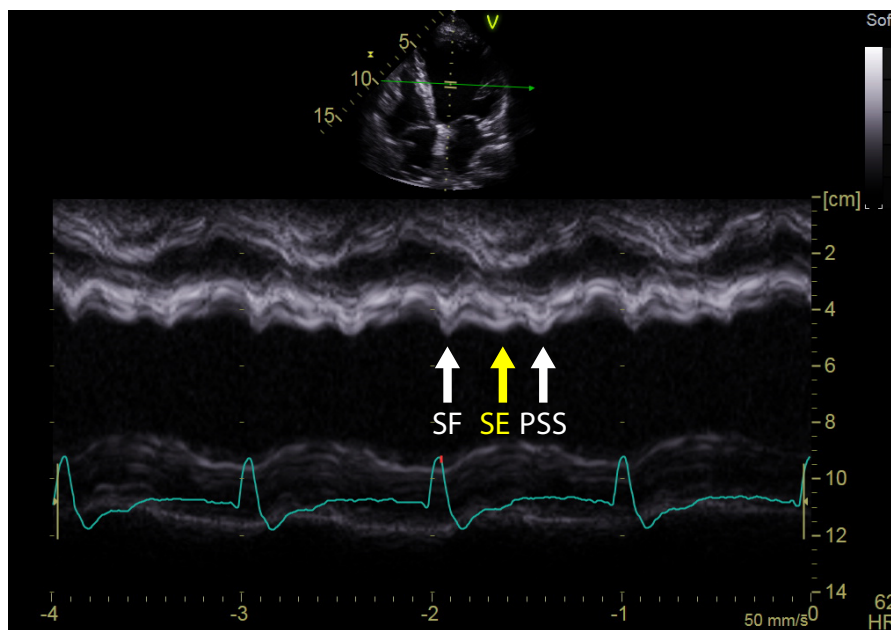
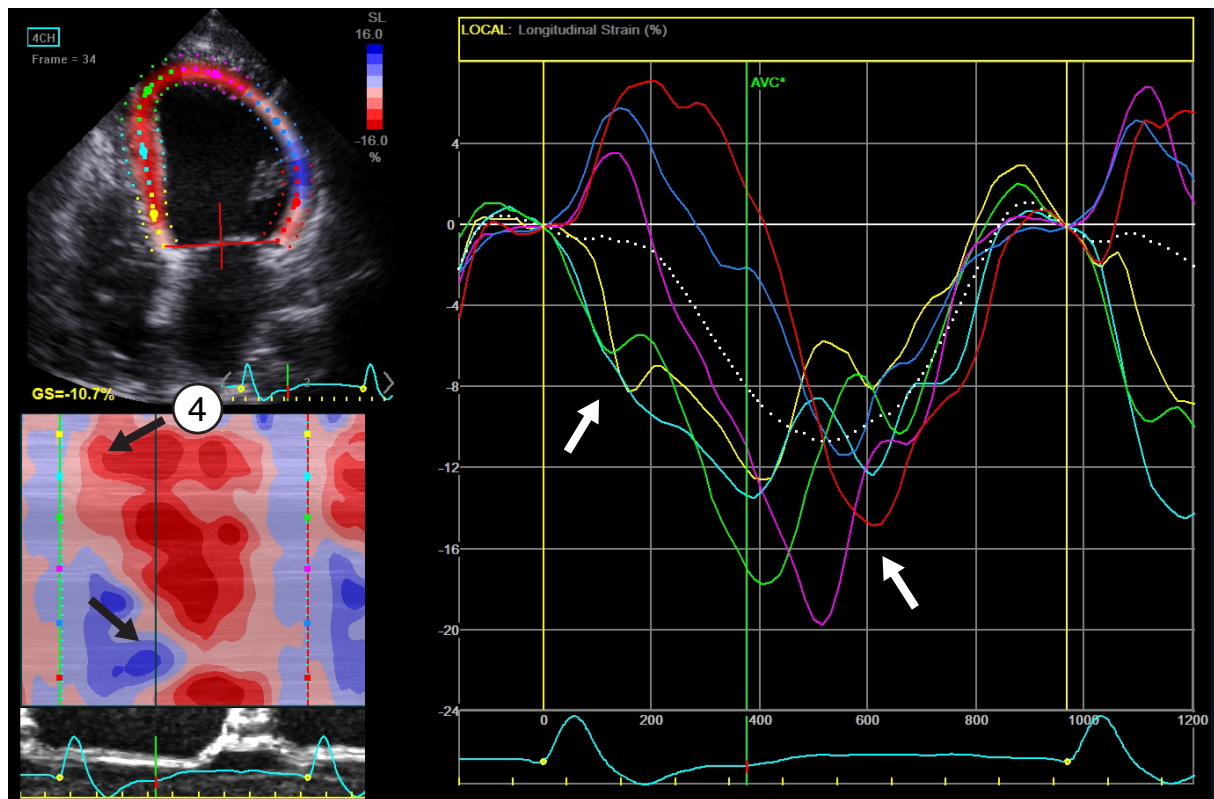


Figure S5

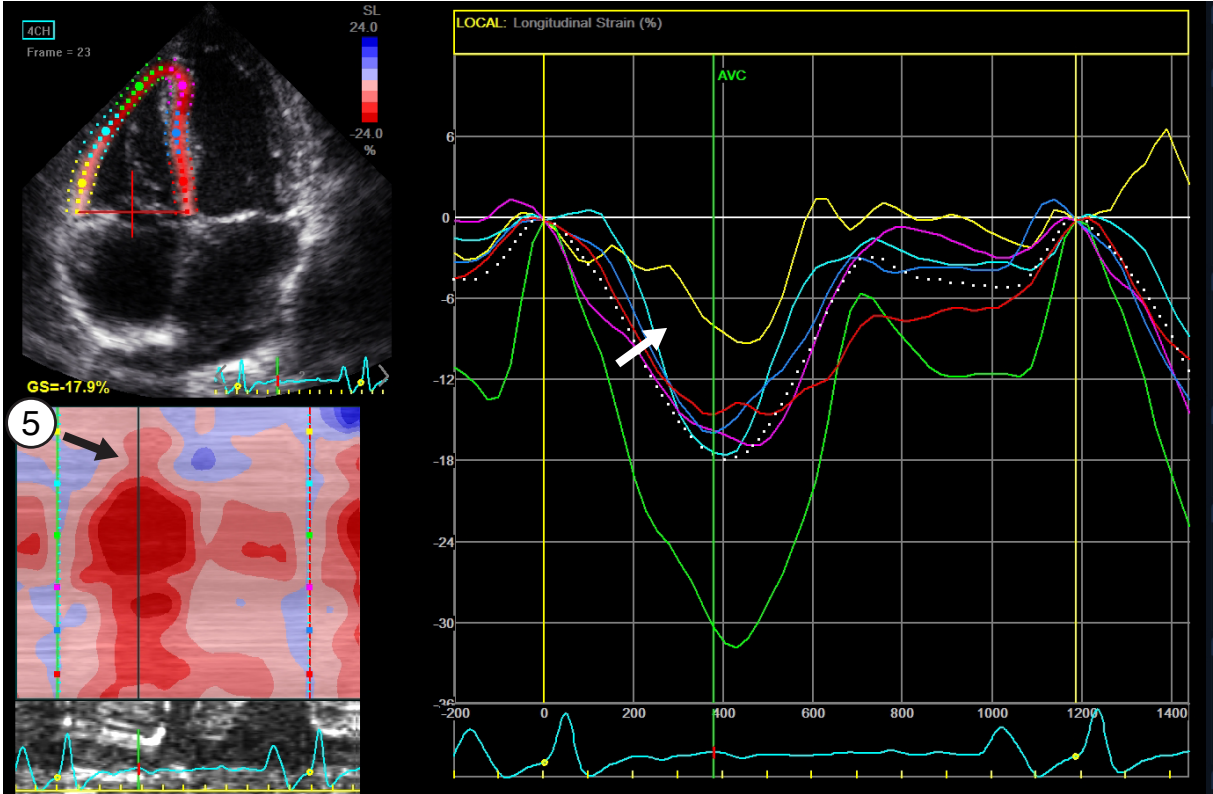


Figure S6

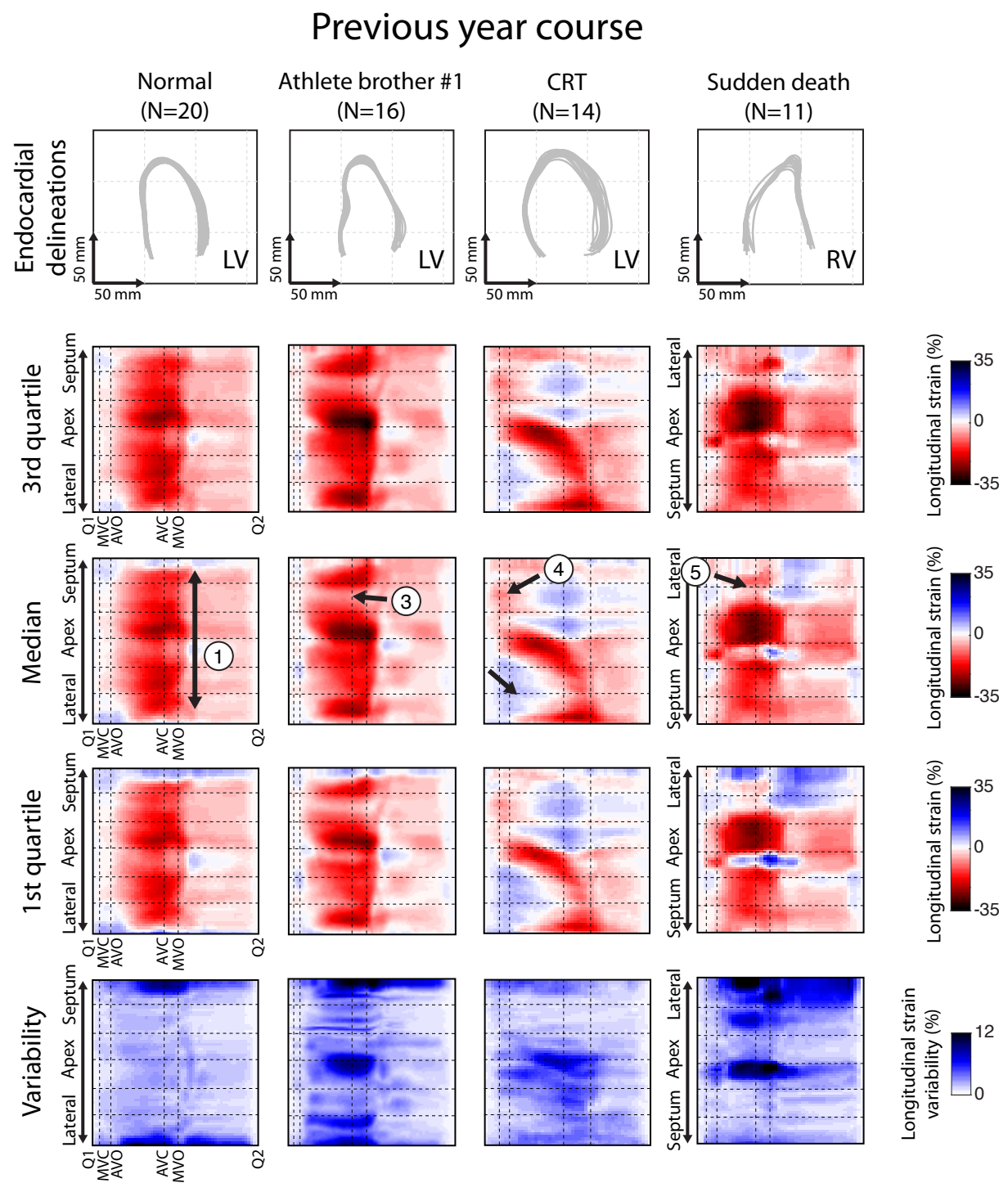


Figure S7

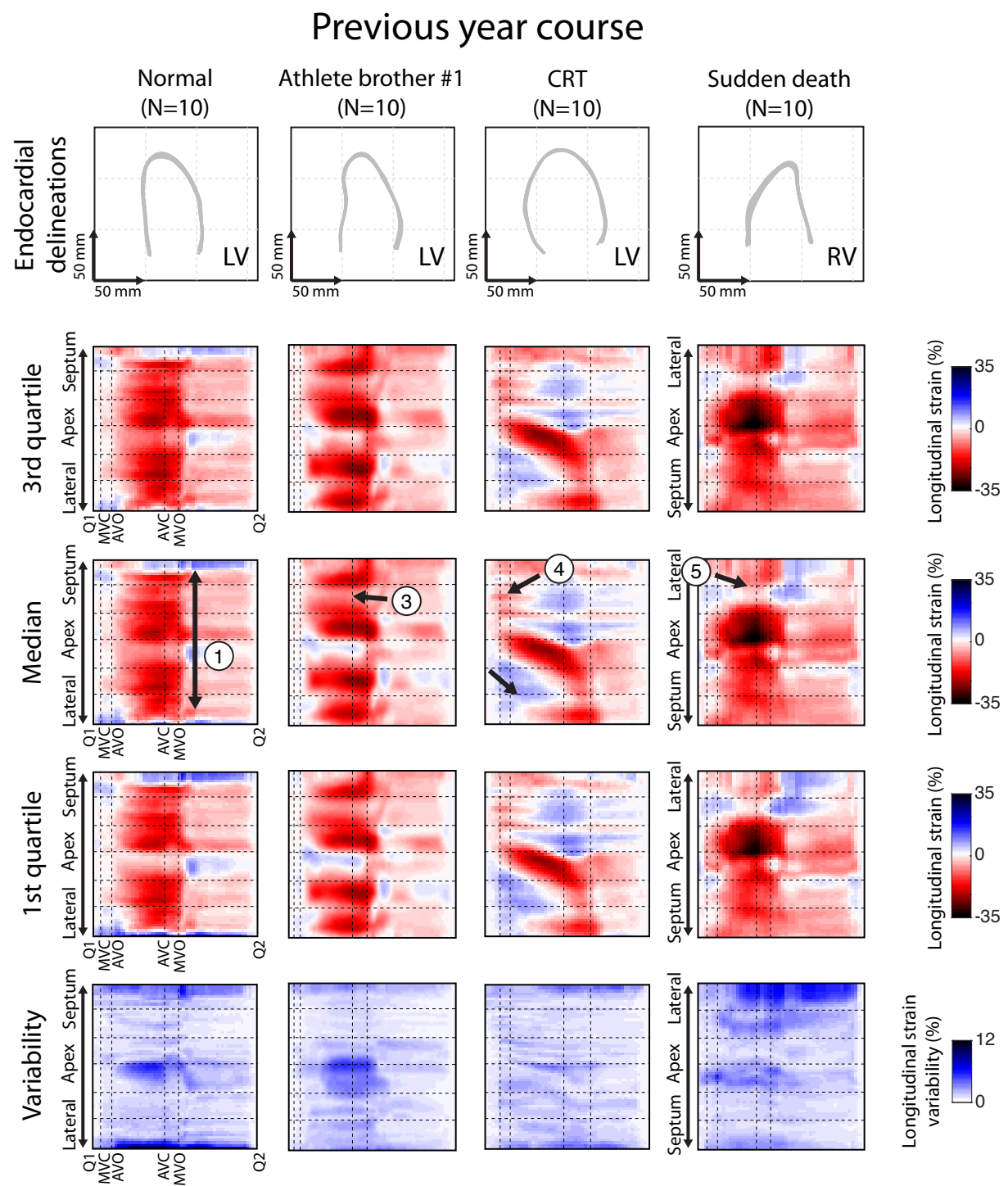


Figure S8

